Signal Transient and Crosstalk Model of Capacitively and Inductively Coupled VLSI Interconnect Lines

Taehoon Kim, Dongchul Kim, and Yungseon Eo

Abstract—**Analytical compact form models for the signal transients and crosstalk noise of inductive-effect-prominent multi-coupled RLC lines are developed. Capacitive and inductive coupling effects are investigated and formulated in terms of the equivalent transmission line model and transmission line parameters for fundamental modes. The signal transients and crosstalk noise expressions of two coupled lines are derived by using a waveform approximation technique. It is shown that the models have excellent agreement with SPICE simulation.**

Index Terms—**Crosstalk, inductance effect, interconnect lines, signal transient, transmission lines.**

I. INTRODUCTION

As the clock frequency of VLSI circuits dramatically increases over several GHz, interconnect lines play a pivotal role in the determination of circuit performance [1, 2]. In the strongly-coupled global interconnect lines, the inductances of the lines have significant effects on the circuits' transient characteristics and coupling noises [3]. In such high-speed integrated circuits, since the signal integrity concerned with interconnect lines cannot be guaranteed without taking inductance-prominent transmission line effects into account, the RLC (resistive, inductive, and capacitive) transmission line model for the accurate signal integrity verification of the circuits becomes essential.

Manuscript received Nov. 3, 2007; revised Dec. 3, 2007.
Department of Electrical and Computer Engineering, Hanyang University, Kyungi-Do 426-791, South Korea
E-mail:thkim@giga.hanyang.ac.kr;dckim@giga.hanyang.ac.kr; eo@giga.hanyang.ac.kr

Since the electromagnetic coupling effects crucially limit integrated circuit performance, they have to be considered in the early phase of circuit design. Up to now, numerous crosstalk models have been developed [4-8]. Traditionally, most of the crosstalk models for the on-chip interconnect lines are based on capacitive coupling effect [4, 5]. It is simply because the RC seems to be more prominent than the "L/R." However, as the circuit switching speed increases, the inductive coupling effect plays an important role. Lorival [9] reported that not only capacitive coupling but also inductive coupling of two coupled lines are very significant by separating the capacitive coupling and inductive coupling. As shown in Fig. 1, the crosstalk voltage can be represented by decoupling the capacitive and inductive coupling voltages

$$V_{crosstalk(RLC)} \approx V_{crosstalk(C)} + V_{crosstalk(L)} . \quad (1)$$

Note, only the capacitive crosstalk noise is not accurate enough to verify the signal coupling noise between lines. Thus, the signal transient of the coupling-aware switching lines and the crosstalk noise of a quiet line cannot be accurately determined without considering the inductive coupling effect.

Recently, there has been a lot of research concerned with coupled RLC line analysis and modeling [6-8]. However, unlike the capacitance-effect-prominent lines (i.e., RC lines), a compact form of model concerned with the signal transients of inductive-effect-prominent coupled lines may not be readily determined since the signal transients of inductance-effect-prominent lines result in complicatedly oscillating non-monotonic wave-shapes.

In this work, at first, assuming (1) linear driver model (i.e., voltage source and source resistance), (2) identical RLC coupled lines, and (3) step input signals, compact

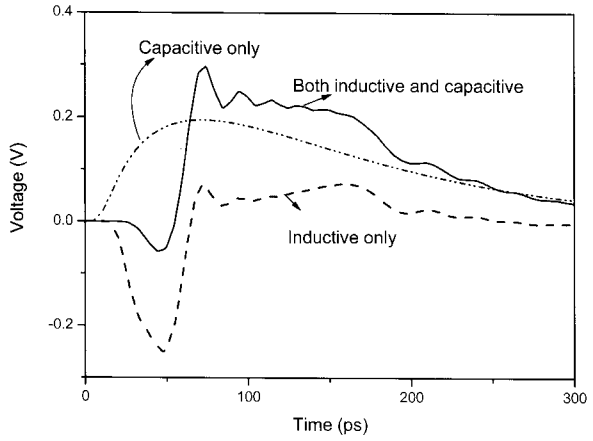

Fig. 1. Inductive and capacitive crosstalk of two coupled lines [9].

closed-form models for signal transients and crosstalk noise of coupled RLC lines are developed and verified. The paper is organized as follows. First, the fundamental modes of the coupled lines and the equivalent transmission line parameters corresponding to the fundamental modes are determined. Next, the analytical models of signal transient and crosstalk noise are developed by using a waveform approximation technique [10]. Finally, it is shown that the developed models have excellent agreement with SPICE simulation.

II. Fundamental Modes of Coupled Interconnect Lines

In the frequency domain, the n-coupled transmission line equations are given by [11],

$$\frac{d^2}{dz^2}[V(z)] = [Z][Y][V(z)], \tag{2}$$

$$\frac{d^2}{dz^2}[I(z)] = [Y][Z][I(z)], \tag{3}$$

where

$$[Z] = [R] + j\omega[L], \tag{4}$$

$$[Y] = [G] + j\omega[C] \approx j\omega[C]. \tag{5}$$

[R], [L], [C], and [G] are PUL (per unit length)-transmission line parameter matrices and are $n \times n$ square matrices. Thus, the system has n eigen modes.

The representative switching patterns of two coupled lines are $0\uparrow$ ($0\downarrow$, $\uparrow 0$), $\uparrow\uparrow$, and $\uparrow\downarrow$, where each switching

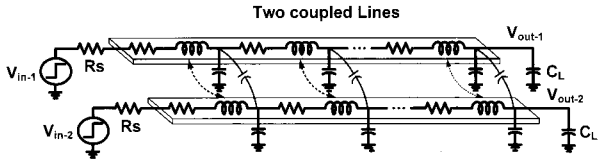

Fig. 2. Two coupled transmission line circuit model.

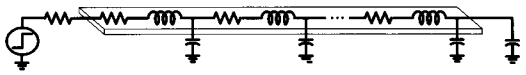

Fig. 3. An equivalent transmission line circuit model for two coupled lines.

characteristic is symbolized and defined by the three switching symbols as $\uparrow$ (switching from logic 0 to logic 1), $\downarrow$ (switching from logic 1 to logic 0), and 0 (the quiet state). However, these switching patterns can be represented by two fundamental switching modes (i.e., even and odd mode). Physically, the even mode is a switching mode in which both lines switch in the same direction (i.e., $\uparrow\uparrow$) and the odd mode means a switching mode in which lines switch in opposite directions (i.e., $\uparrow\downarrow$) [6]. Then the differential equation can be converted to an equivalent single line as shown in Fig. 2 and 3. That is, as an example, the odd mode equation becomes

$$\frac{d^2V_{odd}}{dz^2} = j\omega RC_{odd}V_{odd} - \omega^2 L_{odd}C_{odd}V_{odd}. \tag{6}$$

Thus, once the equivalent transmission line parameters are determined for each fundamental mode, the signal transients and crosstalk can be readily determined.

The per unit length (PUL) transmission line parameters for the identical two coupled lines are defined as

$$[R]_{PUL} = \begin{bmatrix} R & 0 \\ 0 & R \end{bmatrix}, \tag{7}$$

$$[L]_{PUL} = \begin{bmatrix} L_{11} & L_{12} \\ L_{12} & L_{11} \end{bmatrix}, \tag{8}$$

$$[C]_{PUL} = \begin{bmatrix} (C_{11}+C_{12}) & -C_{12} \\ -C_{12} & (C_{12}+C_{11}) \end{bmatrix}. \tag{9}$$

The equivalent transmission line parameters for both the even mode and the odd mode are

$$L_{even} = L_{11} + L_{12},\ C_{even} = C_{11}, \tag{10}$$

$$L_{odd} = L_{11} - L_{12},\ C_{odd} = C_{11} + 2C_{12}. \tag{11}$$

Thus, the characteristic impedances and propagation constants of the even and odd mode can be determined as [9]

$$Z_{even} = \sqrt{\frac{R + j\omega(L_{11} + L_{12})}{j\omega C_{11}}}, \tag{12}$$

$$Z_{odd} = \sqrt{\frac{R + j\omega(L_{11} - L_{12})}{j\omega(C_{11} + 2C_{12})}}, \tag{13}$$

$$\gamma_{even} = \sqrt{(R + j\omega(L_{11} + L_{12}))j\omega C_{11}}, \tag{14}$$

$$\gamma_{odd} = \sqrt{(R + j\omega(L_{11} - L_{12}))j\omega(C_{11} + 2C_{12})}. \tag{15}$$

Note, any signal traveling in the coupled transmission line system can be expressed as the linear combination of these eigen modes. For example, if the first line is switching from logic 0 to logic 1 and the second line is in a quiet state, the signals on the respective lines due to switching (i.e., $\uparrow 0$) can be readily determined by using a symbolic operation

$$(\uparrow 0)_{line-1} \equiv \left(\boxed{\uparrow} 0\right) = \frac{(\uparrow\uparrow) + (\uparrow\downarrow)}{2} = \frac{1}{2}((even) + (odd)) \tag{16}$$

⇨ The switching signal transient of two coupled lines

$$(\uparrow 0)_{line-2} \equiv \left(\uparrow \boxed{0}\right) = \frac{(\uparrow\uparrow) - (\uparrow\downarrow)}{2} = \frac{1}{2}((even) - (odd)) \tag{17}$$

⇨ The crosstalk noise of two coupled lines

Note that the line of interest for the switching mode is marked with a square box.

III. Signal Transient and Crosstalk Models

In order to develop compact analytical models of the coupled interconnect lines, the line driver is modeled with the unit step signal and source resistance while the load is modeled as a capacitance. Then, signal transient and crosstalk noise can be mathematically formulated by using the 3-pole approximation and the modified traveling-wave-based waveform approximation technique (TWA)-based signal transient expressions.

3.1 3-pole Approximation

In the frequency domain, the frequency domain, the transfer function $H(s)$ of the interconnect structure shown in Fig. 4 is given by [10],

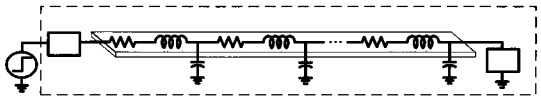

Fig. 4. A simplified circuit model for the interconnect structure.

$$H(s) = \frac{1}{(1 + Zs/Z_L)\cosh(\gamma\ell) + (Zs/Z_0 + Z_0/Z_L)\sinh(\gamma\ell)} \tag{18}$$

where

$$\gamma(s) = \sqrt{(R + sL)sC}\ ,\ Z_0(s) = \sqrt{(R + sL)/sC}. \tag{19}$$

Assuming CMOS digital circuits, the large-signal source impedance can be modeled as a resistive impedance, (i.e., $Zs = Rs$) and the large-signal load impedance is best modeled as a capacitive impedance (i.e., $Z_L = 1/sC_L$). The time-domain step response back into the time domain as

$$V_o(t) = \Im^{-1}\{H(s)V_i(s)\} \tag{20}$$

where $V_i(s)$ is an input step function. Note that a capacitively dominated RLC lines has an RC-like response and can be readily approximated by using three dominant poles [10, 13].

3.2 Traveling-wave-based Waveform Approximation Technique (TWA)

The physical description of the transient signal of a transmission line can be efficiently characterized by using a traveling-wave-based waveform approximation technique which combines a frequency-domain-based approximation for low-frequency characteristics with a time-domain-based approximation for high-frequency characteristics of the system response [10]. In the TWA-technique, assuming

a step input, the low-frequency transient signal is represented with only three-dominant poles. The three-pole-based frequency-domain response function can be transformed back in the time-domain without any numerical integration. Then the high-frequency characteristics of the transient signal are incorporated into an approximation function by exploiting the traveling wave characteristics and a modified-RC-response approximation in the time domain.

When the load is open circuit, the resultant wave shape becomes at double the incident wave. However, a pulsed signal includes many frequency components from dc to very high frequency. Further, since the capacitive reactance of the load is frequency-dependent. That is, with the capacitive load, the refection coefficient is in the range of 1 (for dc) to -1 (for very high-frequency components). This can be represented by combining a linear ramp shape (lower part) with a RC-response-like wave-shape (upper part) since the sharp edge part (i.e., the part that is concerned with the high-frequency components) of the time domain voltage response which is the summation of the incident and reflected waves is blunt a bit. Consequently, the upper part of the resultant response wave-shape is similar to the RC-response-like one, while the lower part of the resultant response wave-shape is similar to a ramp function. In order to separately model the linear ramp shape and RC-response-like shape of the resultant response signal, the boundary point has to be introduced. In practice, the exact boundary point between the linear part and the blunted part may not be accurately determined. Nonetheless, since the blunt amount of the wave-shape is similar to a ramp function. In order to separately model the linear ramp shape and RC-response-like shape of the resultant response signal, the boundary point has to be introduced. In practice, the exact boundary point between the linear part and the blunted part may not be accurately determined. Nonetheless, since the blunt amount of the wave-shape is strongly correlated with the magnitude of the load capacitance, the effect is modeled in terms of the load capacitance. That is, the smaller the load capacitance, the smaller the load capacitance effect. Thus, the capacitive loading effect is modeled as follows. The first incident wave arrives at the load with the time of the flight of a wave that is given by $t_f^- \approx l\sqrt{LC}$. Including the load capacitance C_L, and effective time of flight (t_{f0}) is approximately $t_{f0} \approx l\sqrt{L(C+C_L)}$. Defining the quantity which denotes δ the time difference between the flight time of the pure (unloaded) line and that of the line including loading effects as

$$\delta \equiv l\sqrt{L(C+C_L)} - l\sqrt{LC} \tag{21}$$

the instant right before an incident wave is reflected can be represented by $t_f^- = t_{f0} - \delta$. Note that δ is considered to be an effective response time delay of the incident wave due to the capacitive load. Since the blunt effect of the pulsed signal happens at the upper part of the pulse, it may be assumed that the blunt effect approximately occurs after $t_{f0} + \eta\delta$, where η is a constant factor which has approximately the value of one. In fact, since the RC-like response is approximately linear function until the 63% of the final value, η is not a critical factor to determine the wave-shape. Thus, in this work, it is conveniently selected as $\eta \approx 1$.

Thus, in the time interval between $(2n-1)t_{f0} - \delta$ and $(2n-1)t_{f0} + \delta$, where $n = 1,2,3...$ (note, n is the reflection count), the waveform can be approximated with a linear function. In contrast, in the time interval between $(2n-1)t_{f0} + \delta$ and $(2n+1)t_{f0} - \delta$, the waveform can be modeled with an RC-response-like function. The time constant for this "fictitious" charging or discharging can be estimated by using an effective RC time constant (including C_L) of the system. The fictitious charging or discharging time constant τ can be reasonably modeled as $\tau = (l \cdot R)(l \cdot C + C_L)$.

TWA-based resultant waveform is given by [10]. For $(2n-1)t_{f0} - \delta \le t \le (2n-1)t_{f0} + \delta$, the response can be modeled as linear ramp shape, as

$$V_o(t) \approx \sum_{n=1}^{\infty} \left[\left\{ \frac{V_{3pole}\left((2n-1)t_{f0}\right) - V_{3pole}\left(2(n+1)t_{f0} + \delta\right)}{\delta} \left(t - (2n-1)t_{f0}\right) \right\} + V_{3pole}\left((2n-1)t_{f0}\right) \right] \cdot \left[u\left(t - 2(n-1)t_{f0} + \delta\right) - u\left(t - 2(n-1)t_{f0} - \delta\right) \right] \tag{22}$$

while, for $(2n-1)t_{f0} + \delta \le t \le (2n+1)t_{f0} - \delta$, the response can be modeled as RC-response-like shape

$$V_o(t) \approx \sum_{n=1}^{\infty} \left[\begin{array}{l} 2V_{3pole}\left((2n-1)t_{f0}\right) - V_{3pole}\left(2(n+1)t_{f0} - \delta\right) \\ +\omega_n \left\{ 1 - \exp\left(-\dfrac{t-(t_{f0}+\delta)}{\tau} \right) \right\} \end{array} \right] \cdot \left[u\left(t - 2(n-1)t_{f0} - \delta\right) - u\left(t - 2(n+1)t_{f0} + \delta\right) \right] \quad (23)$$

where

$$\omega_n = \frac{V_{3pole}\left(2nt_{f0} + t_f^-\right) - 2V_{3pole}\left((2n-1)t_{f0}\right)}{1 - \exp\left\{ -\dfrac{2(t_f^-)}{\tau} \right\}} + \frac{V_{3pole}\left((2n+1)t_{f0} + t_f^-\right)}{1 - \exp\left\{ -\dfrac{2t_f^-}{\tau} \right\}} \quad (24)$$

In the expressions, V_{3pole} is the three-pole-based time-domain response function and n indicates n th reflection. Thereby, an accurate time domain response signal can be calculated. Note, the magnitude of the overshoot/ undershoot can be readily determined by using (23) since the overshoot /undershoot alternately occur in the time interval of $(2n-1)t_{f0} + \delta \le t \le (2n+1)t_{f0} - \delta$.

3.3 Compact Analytical Models

For on-chip interconnects, in the odd mode, the relation $R >> \omega L_{odd}$ is generally verified [9]. Thus, for simplicity, the odd mode waveform (V_{odd}) can be approximately determined only with 3-poles.

$$V_{odd}(0 \le t \le \infty) \approx V_{3pole}^{odd}(t) \quad (25)$$

The subscript "3pole" indicates the three-pole-based time-domain response.

Unlike the odd mode signals, the even mode signals have significant inductance effects. So, in this case, the modified TWA technique is employed. The time of flight (t_{f0}^{even}) and a time difference with the wave reflection (δ_{even}) for the even mode are defined as

$$t_{f0}^{even} = \sqrt{l \cdot L_{even}(l \cdot C_{even} + C_L)}, \quad (26)$$

$$\delta_{even} = \sqrt{l \cdot L_{even}(l \cdot C_{even} + C_L)} - l\sqrt{L_{even}C_{even}}. \quad (27)$$

Thus, for the even mode, the waveform can be determined as

$$V_{even}(0 \le t < (t_{f0}^{even} - \delta_{even})) = 0, \quad (28)$$

$$V_{even}((t_{f0}^{even} - \delta_{even}) \le t \le (t_{f0}^{even} + \delta_{even})) = \frac{V_{3pole}^{even}(t_{f0}^{even})}{\delta_{even}}(t - t_{f0}^{even}) + V_{3pole}^{even}(t_{f0}^{even}), \quad (29)$$

$$V_{even}((t_{f0}^{even} + \delta_{even}) \le t \le (3t_{f0}^{even} - \delta_{even})) = 2V_{3pole}^{even}(t_{f0}^{even}) + \omega_{even}\left[1 - \exp\left\{ -\frac{t - (t_{f0}^{even} + \delta^{even})}{\tau_{even}} \right\} \right], \quad (30)$$

where

$$\tau_{even} = (l \cdot R)(l \cdot C_{even} + C_L), \quad (31)$$

$$\omega_{even} = \frac{V_{3pole}^{even}(3t_{f0}^{even} - \delta_{even}) - 2V_{3pole}^{even}(t_{f0}^{even})}{1 - \exp\left\{ -\dfrac{2(t_{f0}^{even} - \delta_{even})}{\tau_{even}} \right\}}. \quad (32)$$

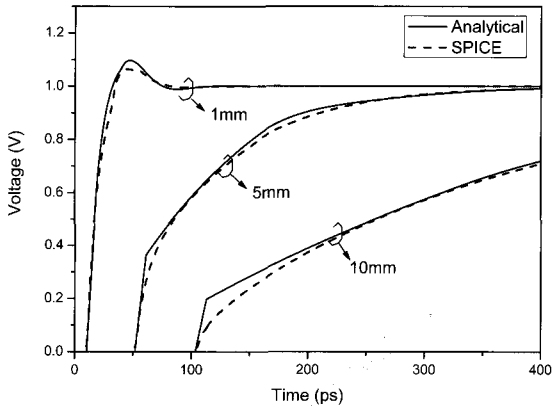

(a) Even mode

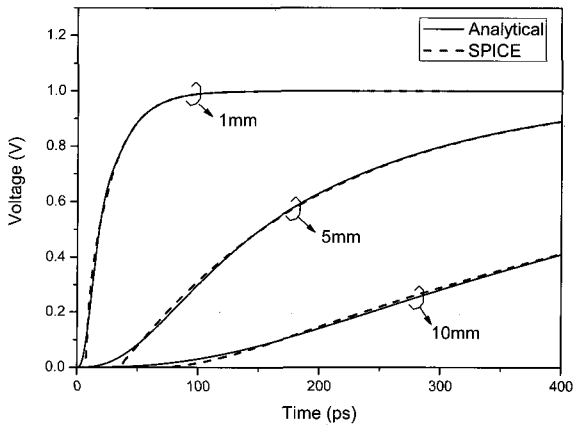

(b) Odd mode

Fig. 5. Signal transient comparison of analytical models and SPICE simulations for the fundamental modes of 2-coupled lines.

Since the far end reflection wave after three time of flight may be not significant, the even mode can be approximated as

$$V_{even}(t \geq (3 \cdot t_{f0}^{even} - \delta_{even})) \approx V_{3pole}^{even}(t \geq (3 \cdot t_{f0}^{even} - \delta_{even})). \quad (33)$$

Fig. 5 shows comparisions of compact analytical models and SPICE simulations for even and odd mode.

IV. Verification of the Models

In order to verify the accuracy of the proposed model, transmission line parameters are determined for test structures (see Fig. 6) by using a commercial field solver. Test structures are based on a DSM (deep submicron) technology [1], [12]. The transmission line parameters for two coupled lines are

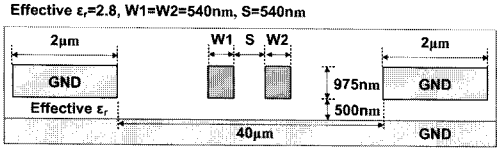

Fig. 6. Test circuit structure.

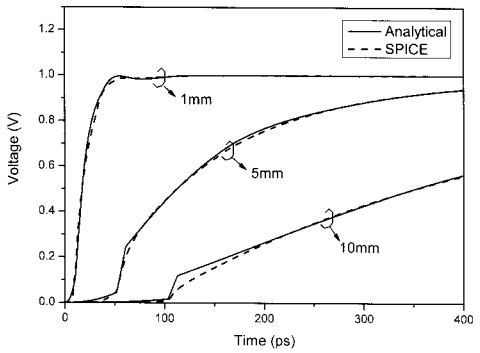

(a) Signal transient (↑0)

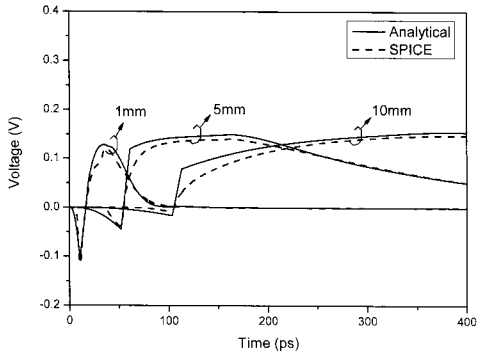

(b) Crosstalk (↑0)

Fig. 7. Signal transient comparison of analytical models and SPICE simulations for the various lengths.

$$[R] = \begin{bmatrix} 44.44 & 0 \\ 0 & 44.44 \end{bmatrix} \left[\frac{\Omega}{mm}\right], \quad (34)$$

$$[L] = \begin{bmatrix} 0.612 & 0.380 \\ 0.380 & 0.612 \end{bmatrix} \left[\frac{nH}{mm}\right], \quad (35)$$

$$[C] = \begin{bmatrix} 161.83 & -54.884 \\ -54.884 & 161.83 \end{bmatrix} \left[\frac{fF}{mm}\right]. \quad (36)$$

As shown in Fig. 7, signal transients and crosstalk noise using the proposed compact models are compared with the SPICE simulation. The proposed models have excellent agreement with SPICE simulation.

V. Conclusions

In this work, compact analytical models for the signal transients and crosstalk noises of coupled RLC transmission lines are developed. The coupled lines are decoupled with fundamental modes and then their signal transients and crosstalk noise are determined by using "traveling-wave-based waveform approximation" which is a kind of closed-form model. Since a switching pattern for the coupled lines can be readily decomposed with the fundamental modes, the signal transients and crosstalk can be very efficiently determined. It was shown that the developed compact models have excellent agreement with SPICE simulation.

References

[1] "International Technology Roadmap for Semiconductors," *SIA Report*, 2006.

[2] A. Deutsch et al., "On-chip wiring design challenges for gigahertz operation," *Proc. IEEE*, vol. 89, no. 4, pp. 529-555, Apr. 2001.

[3] Y. Massoud and Y. Ismail, "Grasping the impact of on-chip inductance," *IEEE Circuits and Devices*, vol. 17, no. 4, pp. 14-21, Jul. 2001.

[4] T. Sakurai, "Closed-form expressions for interconnection delay, coupling, and crosstalk in VLSI's," *IEEE Trans. Electron Devices*, vol. 40, no.1, pp.118-124, Jan. 1993.

[5] J. Zhang and E. G. Friedman, "Effect of shield insertion on reducing crosstalk noise between coupled

interconnects," in *IEEE Int. Symp. on Circuit and Systems*, pp. 529-532, 2004.

[6] K. Agarwal, D. Sylvester, and D. Blaauw, "Modeling and analysis of crosstalk noise in coupled RLC interconnects," *IEEE Trans. Computer-Aided Design*, vol. 25, no. 5, pp. 892-901, May 2006.

[7] J. E. Lorival et al., "Analytical expressions for capacitive and inductive coupling," in *IEEE Workshop on SPI*, pp. 115-118, 2006.

[8] L.Yin and L. He, "An efficient analytical model of coupled on-chip RLC interconnects," in *Proc. ASP-DAC*, pp. 385-390, 2001.

[9] J. E. Lorival, D. Deschacht, Y. Quere, T. L. Gouguec, and F. Huret, "Additivity of capacitive and inductive coupling in submicronic interconnects," in *IEEE DTIS*, pp. 300-304, 2006.

[10] Y. Eo, J. Shim, and W. R. Eisenstadt, "A traveling-wave-based waveform approximation technique for the timing verification of single transmission lines," *IEEE Trans. Computer-Aided Design*, vol. 21, no. 6, pp. 723-730, June 2002.

[11] C. R. Paul, Analysis of Multiconductor Transmission Lines. New York: Wiley, 1994.

[12] P. Bai et al., "A 65nm logic technology featuring 35nm gate lengths, enhanced channel strain, 8 Cu interconnect layers, low-k ILD and 0.57μm2 SRAM cell" in *IEEE Int. Electron Device Meeting*, pp. 657- 660, 2004.

[13] Y. I. Ismail, Eby. G. Friedman, and Jose L. Neves, "Figures of merit to characterize the importance of on-chip inductance," *IEEE Trans. VLSI.*, vol. 7, no. 4, pp. 442-449, Dec. 1999.

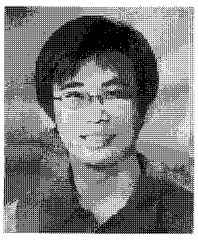

Taehoon Kim received his B.S. in electrical and computer engineering from Hanyang University, Korea in 2007. He is currently working toward his M.S and Ph.D. in Electrical and Computer Engineering at Hanyang University, Ansan, Korea. His research interests are high-frequency characterization, modeling, and simulation concerned with the signal integrity verification of high-speed integrated circuits, IC interconnects, and IC packaging.

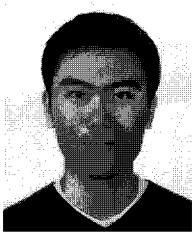

Dongchul Kim received his B.S. in electrical and computer engineering from Hanyang University, Korea in 2007. He is currently working toward his M.S. and Ph.D in Electrical and Computer Engineering at Hanyang University, Ansan, Korea. His research interests include high-frequency characterization, modeling, and simulation concerned with the signal integrity verification of high-speed, VLSI circuits and intergrated circuit packaging.

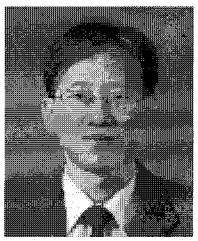

Yungseon Eo received his B.S. and M.S. in electronic engineering from Hanyang University, Seoul, Korea, in 1983 and 1985, respectively, and his Ph.D. in Electrical Engineering from the University of Florida, Gainesville, FL, in 1993. From 1986 to 1988, he was with the Korea Telecommunication Authority Research Center, Seoul, where he performed telecommunication network planning and software design. From 1993 to 1994, he was with Applied Micro Circuits Corporation, San Diego, CA., where he performed s-parameter-based device characterization and modeling for high-speed circuit design. From 1994 to 1995, he was with the Research and Development Center of LSI Logic Corporation, Santa Clara, CA, where he worked in the signal integrity characterization and modeling of high-speed CMOS circuits and interconnects. From 2004 to 2005, he was with High-Speed Microelectronics Group as a guest researcher at the National Institute of Standards and Technology (NIST), Boulder, CO. He is now a Professor of Electrical and Computer Engineering at Hanyang University, Ansan, Korea. His research interests are high-frequency characterization, modeling, and simulation methodology concerned with integrated circuits interconnects, integrated circuit packaging, and system level integration technology.